Karyopherin MoKap119-mediated nuclear import of cyclin dependent kinase regulator MoCks1 is essential for Magnaporthe oryzae pathogenicity

Article *in* Cellular Microbiology · September 2019

DOI: 10.1111/cmi.13114

5 authors, including:

Shulin Zhang
Guangdong Academy of Agricultural Sciences
7 PUBLICATIONS **53** CITATIONS

SEE PROFILE

Deng Yizhen (Orcid ID: 0000-0002-3572-1559)

Karyopherin MoKap119-mediated nuclear import of cyclin dependent kinase regulator MoCks1 is essential for *Magnaporthe oryzae* pathogenicity

Shulin Zhang[1,2#], Chaoxiang Lin[1,2#], Tian Zhou[1,2], Lian-Hui Zhang[1,2*], Yi Zhen Deng[1,2*]

1. Key Laboratory for Conservation and Utilization of Subtropical Agro-Bioresources, College of Agriculture, South China Agricultural University, Guangzhou, Peoples' Republic of China 510642.

2. Integrative Microbiology Research Centre, South China Agricultural University, Guangzhou, Peoples' Republic of China 510642.

Co-first authors.

* Address correspondence to YZ Deng (email: dengyz@scau.edu.cn) and LH Zhang (lhzhang01@scau.edu.cn).

This article has been accepted for publication and undergone full peer review but has not been through the copyediting, typesetting, pagination and proofreading process which may lead to differences between this version and the Version of Record. Please cite this article as doi: 10.1111/cmi.13114

Abstract

Nuclear import of proteins relies on nuclear import receptors called importins/karyopherins (Kaps), whose functions were reported in yeasts, fungi, plants and animal cells, including cell cycle control, morphogenesis, stress sensing/response, and also fungal pathogenecity. However, limited is known about the physiological function and regulatory mechanism of protein import in the rice-blast fungus *Magnaporthe oryzae*. Here, we identified an ortholog of β-importin in *M. oryzae* encoded by an ortholog of *KAP119* gene. Functional characterization of this gene via reverse genetics revealed that it is required for vegetative growth, conidiation, melanin pigmentation and pathogenicity of *M. oryzae*. The *mokap119*Δ mutant was also defective in formation of appressorium-like structure from hyphal tips. By affinity assay and LC-MS/MS, we identified potential MoKap119-interacting proteins, and we further verified that MoKap119 interacts with the cyclin dependent kinase subunit MoCks1 and mediates its nuclear import. Transcriptional profiling indicated that MoKap119 may regulate transcription of infection-related genes via MoCks1-regulation of MoSom1. Overall, our findings provide a novel insight into the regulatory mechanism of *M. oryzae* pathogenesis likely by MoKap119-mediated nuclear import of the cyclin dependent kinase subunit MoCks1.

Introduction

Phytopathogenic fungi, compared with oomycete and bacterial pathogens, cause more serious yield losses in agricultural practice [1]. Among all crop fungal pathogens, the hemi-biotrophic ascomycete *Magnaporthe oryzae* causes rice-blast disease leading to 10-30% yield losses worldwide [2], and therefore is reported as the number 1 of the top 10 fungal pathogens [3]. *M. oryzae* produces the asexual spores named conidia, to spread and get contact with the host rice [4]. The conidia germinate and differentiate into a dome-shaped structure called appressorium to facilitate host invasion by generating high pressure turgor within its vacuolar lumen [5,6]. Genes essential for *M. oryzae* conidiation have been identified, including *MoCDC15*, *MoCHS1*, and *MoCOM1* etc [7-9]. Signal transduction pathways, including G-protein signaling pathway, cAMP-PKA signaling pathway, MAPK signaling pathway etc [10-12], have also been characterized in *M. oryzae* during host-infection stages. These reports demonstrate the importance of transducing environmental/intracellular signals to nuclear transcription factors, culminating in altered expression of target genes to promote cellular differentiation, yet limited is known about how such nuclear import of signal transducer(s) is regulated in *M. oryzae* [13].

Nucleocytoplsmic shuttling of such signal transducers/proteins takes place through the nuclear pore complex (NPC) [14], and is mediated by nucleocytoplasmic transport receptors (NTRs), comprised of β-importin and α-importin (also called karyopherin-β or karyopherin-α) subunits. β-Importin can form heterodimers with α-importin, in which

β-importin mediates interactions with the NPC, while α-importin binds the nuclear localisation signals (NLSs) of the cargo proteins. Members of the β-importin family can also interact with NLSs or nuclear export signals (NESs) of some cargoes for their nuclear transport or export [15]. The budding yeast *Saccharomyces cerevisiae* contains 1 α-importins and 14 β-importins, likely serving differential cargo recognition and transport functions [16]. Some of the yeast β-importins have been well characterized in terms of their cargo and biological function, e.g. β-importin ScNmd5 (Kap119) is required for nuclear import of Hog1 MAPK, under osmotic stress [17], and also for the transcription factor TFIIS [18]; β-importin Kap95 mediates nuclear imported of Mig2 transcriptional factor for glucose repression of the *SUC2* gene [19], of Slt2 kinase and Rlm1 transcription factor responsible for cell wall integrity [20], and of Swi6 for cell cycle progress [21]; β-importin Msn5 mediates nuclear export of cell cycle transcription factor Swi5 by direct binding to its N-terminus [22]. In filamentous fungi, systematic functional and localization analyses were performed in *Aspergillus nidulans*, identifying 14 karyopherins (KAPs) belonging to the karyopherin-β superfamily. Except for 4 *KAP* genes that may be essential and thus the deletion mutants were not available, most of the rest single-gene deletion mutants displayed no obvious phenotype, indicating redundant roles for these KAPs [23]. Among them, the β-importin KapI (homologous to yeast Kap121) controls colonial and asexual development in *A. nidulans* [24], and the α-importin KapA is required for proper sexual and asexual development and secondary metabolism [25]. Recently, it has been reported that α-importin mediates nuclear transport of NIT-2 transcription factor in *Neurospora crassa* [26], and β-importin Kap8 mediates cellulase transcriptional regulator XYR1 in *Trichoderma reesei* [27]. *M. oryzae*

ortholog of exportin-5/Msn5p (EXP5) has been identified and was shown to be required for producing necrotic symptoms on roots [13], but the exact mechanism including substrate protein(s) is not clear. None of other importins has been identified or characterized in *M. oryzae*.

Given that ScNmd5/Kap119 was reported to be responsible for nuclear import of Hog1 [17], and *M. oryzae* Hog1 is important for conidia production [28], we chose to identify the *M. oryzae* ortholog of ScNmd5/Kap119 and tried to investigate its function. In this study, we identified an ortholog of β-importin ScNmd5/Kap119, encoded by *MGG_02927* in *M. oryzae*, and named it as MoKap119. By reverse genetics and detailed biochemical analysis we characterized the function of MoKap119 in *M. oryzae* development and pathogenic differentiation. Our results demonstrated that MoKap119 regulates *M. oryzae* vegetative growth, asexual differentiation and pathogenicity, like via mediating nuclear import of the cyclin dependent kinase subunit MoCks1, an important regulators of fungal differentiation.

Results

Identification and deletion of *MoKAP119* gene

We set up to study biological function and mechanism of nucleocytoplsmic shuttling of proteins mediated by karyopherins in *M. oryzae*. Using the *S. cerevisiae* ScNmd5/Kap119 protein sequence as a query to search the *M. oryzae* genome database in FungiDB

(http://fungidb.org), we identified an orthologue protein (XP_003720790.1) encoded by gene *MGG_02927*, which comprises an open read frame (ORF) of 3162 bp with 7 introns. Phylogenetic analysis with the yeast/fungal, animal and plant orthologs of MGG_02927 protein showed that it is highly conserved among fungi (Fig. 1A). Given that the closest characterized orthologs of MGG_02927 comes from *T. reesei* or *A. nidulans*, in which this protein was named Kap119, we here named it as MoKap119. The plant or animal β-importin sequences from BLASTP search using MoKap119 as a bait were clustered in two seperated clades, with exception of *Quercus suber* (plant), which is clustered into fungal clade (Fig. 1A, asterisk). The amino acid sequence of MoKap119 was aligned with the orthologs of *S. cerevisiae*, *A. nidulans* and *T. reesei* as shown in Figure 1B. The Importin-beta N-terminal domain (IBN _N) was highly conserved in these 4 aligned Kap119 proteins (Fig. 1B).

For functional characterization, we generated the targeted gene deletion mutant of *MoKAP119* using homologous recombination strategy (Fig. S1A), and three *mokap119*Δ mutants, #4, #9 and #16 were verified by PCR (Fig. S1B). The *MoKAP119* gene complementation was constructed and transformed into the *mokap119*Δ mutant (#9), to generate the complementation strain D9-C, which was verified by Southern blot (Fig. S1C) and RT-PCR (Fig. S1D). The *mokap119*Δ mutants D4 and D9, as well as the complementation strain D9-C1 and D9-C2 were used for assessment in vegetative growth, conidiation, and host infection as follows. Representative results were displayed.

***MoKAP119* is important in mycelial growth and pigmentation**

First we assessed the mycelial growth with the wild type (WT), *mokap119*Δ mutants and the complemented strains on complete medium (CM). The *mokap119*Δ mutant displayed a significant reduction in radial growth compared to the WT and the complemented strain (Fig. 2A-B). In addition, we noticed that the *mokap119*Δ mutant colony appeared less pigmented compared to the WT and the complemented strain (Fig. 2A, lower panel). As expected, the expression of three pigmentation biosynthesis genes *BUF1*, *ALB1* and *RSY1* [29] was significantly reduced in the mutant (Fig. 2C). We conclude that *MoKAP119* is involved in *M. oryzae* vegetative growth and mycelial pigmentation, likely by regulating expression of genes essential for melanin biosynthesis.

***MoKAP119* is required for conidiation**

Next we investigate conidiation in the WT, *mokap119*Δ mutants and the complemented strains. We found that the *mokap119*Δ mutant produced no conidia under inductive condition when cultured on prune juice agar (PA) medium (Fig. 2D). For better visualization of conidia formation, we attached the glass slides to the cultured mycelial plugs and allowed the cultures to grow under light for 24 h. Under microscope, we observed numerous conidia produced by the WT and the complemented strain (Fig. 2E). In contrast, none conidia were formed in the *mokap119*Δ mutant (Fig. 2E). These results confirmed that *MoKAP119* is essential for *M. oryzae* conidiation.

***MoKAP119* is indispensable for *M. oryzae* pathogenicity**

To evaluate the role of *MoKAP119* in pathogenicity, we performed plant infection assays on detached susceptible barley and rice leaves with mycelial agar plugs, due to unavailability of the *mokap119*Δ conidia. After 5 day post inoculation (dpi), typical blast lesions were developed on both susceptible barley and rice leaves inoculated with WT or the complemented strain, while no lesion on the leaves inoculated with the mutant (Fig. 3A). The *mokap119*Δ mutant was non-pathogenic even by inoculating on the wounded barley leaves (Fig. 3A, denoted by "W"). We also performed rice root infection assay. Consistently, the *mokap119*Δ mutant was unable to cause blackening/lesion, as a symptom of infection, to the rice roots, while WT and the complemented strain could (Fig. 3B, arrows).

It has been reported that an appresorium-like structure could be formed from *M. oryzae* mycelial tips and mediated host penetration and infection [30]. Therefore we examined the formation of such appressorium-like structure in the *mokap119*Δ mutant in comparison to WT and the complemented strain. When inoculated on hydrophobic GelBond film surface with the vegetative mycelia, the appressorium-like structure formed in WT and the complemented strain at 24-48 hpi, while no such appressorium-like structure was observed at the hyphal tips of the *mokap119*Δ mutant (Fig. 3C). Overall, we conclude that *MoKAP119* is essential for appressorium-like structure formation and for *M. oryzae* pathogenicity.

MoKap119 shuttles between Cytoplasm and nucleus

The genetic complementation of *MoKAP119* was constructed with a GFP-tag at its C-terminus therefore the complementation strains D9-C1 and D9-C2 could be used for observing sub-cellular localization of MoKap119 protein. Under epifluorescence microscopy, we observed that MoKap119-GFP signal localized in both cytoplasm and nucleus in conidia, which could be confirmed by co-staining of the nucleus with the fluorescent dye Hoechst 33342 (Fig. 4A). We also examined the sub-cellular localization of MoKap119-GFP during appressorium formation and *in planta* growth. We found that MoKap119-GFP mainly localized in conidial nuclei at the later stage of appressorium formation (Fig. 4A, 12 h). MoKap119-GFP was distributed in both cytosol and nuclei of invasive hypase, formed in the inoculated barely epidermis at 36-48 hpi, as shown in Figure 4B. These results indicated that MoKap119 is dynamically localized in cytoplasm and nucleus, during pathogenic differentiation of *M. oryzae*.

MoKap119 is essential for nuclear import of the CDK regulator MoCks1

To identify potential cargo or partner proteins of MoKap119, we enriched its interacting protein by affinity assay and identified such interacting proteins by mass spectrometry analysis. The LC-MS/MS analysis identified 996 proteins in total, with 1-41 unipeptides per protein (Suppl Dataset 1). The top identified protein was MoKap119, used as a bait for the affinity assay, with the most unipeptide counts (41, Suppl Dataset 1), suggesting that our result was reliable. KEGG analysis showed that MoKap119-interacting proteins were

enriched in RNA transport, protein or amino acid metabolism or degradation, carbon metabolism, oxidative phosphorylation, and MAPK signaling pathways (Fig. S2 and Suppl Dataset 2). We were interested to notice that 15 proteins of MAPK signaling pathways were shown to interact with MoKap119 (Suppl Dataset 2), and they possibly depend on MoKap119 for their nuclear import. Particularly, the CDK (cyclin dependent kinase) protein Cdc28/Cdc2 (uniprot ID: G4MZ20) at downstream of multiple MAPK signaling pathways, was among the MoKap119-interacting proteins (Fig. S3 and Suppl Dataset 2).

MoCDC28 may be an essential gene therefore its deletion mutant is not available. A recently reported CDK regulator MoCks1 could directly interact with MoCdc28 in nucleus, to regulate *M. oryzae* pathogenicity [31]. Deletion of *MoCKS1* gene resulted in similar phenotypes [31] as *mokap119*Δ mutant, including reduced radial growth, loss of conidiation and the ability to infect the barley or rice leaf explants (with mycelial plugs), and likely due to the loss of MoCks1-regulation of MoCdc28 function [31]. MoCks1 was also shown to interact with the transcriptional factor MoSom1, thus likely regulated transcription of gene essential for *M. oryzae* infection [31]. Since we were unable to generate the *mocdc28*Δ mutant for a further investigation, and the reported *mocks1*Δ and *mosom1*Δ mutants showed similar phenotypes as the *mokap119*Δ mutant did, we hypothesized that MoKap119 may mediate nuclear import of (any one of, or some of) MoCdc28, MoCks1, and MoSom1.

First we performed a yeast-two-hybrid assay to verify the direct interaction of MoKap119 with MoCks1, MoSom1 and MoCdc28 respectively. Our results showed that MoKap119 could directly interact with MoCks1 and MoSom1 (Fig. 5A). However, no direct interaction was detected between MoKap119 and MoCdc28 by yeast-two-hybrid assay (Fig. 5A). We further performed Co-IP assay, and found that MoKap119 could physically interact with MoCdc28 (Fig. 5B). We infer that the discrepancy between affinity assay and the yeast-two-hybrid assay may be due to that interaction between MoKap119 and MoCdc28 does not occur under the standard culture condition used for the yeast-two-hybrid analysis.

We further investigated whether MoCks1, MoCdc28 or MoSom1 depends on MoKap119 for its nuclear import, by tagging each protein with GFP, and observed its subcellular localization in WT or the *mokap119*Δ mutant. Our result showed that MoCdc28-GFP distributed in cytosol as well as in nuclei in both WT and the *mokap119*Δ mutant mycelia (Fig. 6). In contrast, MoCks1-GFP lost its nuclear localization in the *mokap119*Δ mutant, while it localized in both cytosol and nuclei in the WT mycelia (Fig. 6). MoSom1 localized mostly in nuclei, in either WT or the *mokap119*Δ mutant (Fig. 6), indicating that MoKap119 is not required for MoSom1 nuclear import. We further assessed the dependence on MoKap119 importin, for the sub-cellular localization of the Cyclin B proteins, which have been reported essential for MoCks1 function [32]. Three Cyclin B genes were identified in *M. oryzae* genome, including the Cyclin B or B1 (*MGG_05646*, *MGG_07065* and *MGG_03595*). Each Cyclin B protein were tagged with C-terminal GFP and expressed in WT or the *mokap119*Δ

mutant. By epifluorescence microscopy we observed that Cyclin B (MGG_07065) or B1 protein (MGG_03595) localized in both cytosol and nucleus and Cyclin B (MGG_05646) was enriched in nucleus. However, MoKap119 was not required for maintaining the sub-cellular localization of these three Cyclin B proteins as their localization was comparable in WT and the mutant (Fig. 7). Overall we conclude that MoKap119 directly interacts with MoCdc28, MoCks1 and MoSom1, and essential for nuclear import of MoCks1 in *M. oryzae*. However it was not involved in regulating sub-cellular localization of MoCdc28, MoSom1 or Cyclin B proteins.

MoKap119 may regulate transcription of infection-related genes via MoCks1 regulation of MoSom1

We noticed that the reported phenotypes of *mosom1*Δ mutant [33] also mimics the *mokap119*Δ mutant. Given that MoCks1 depends on MoKap119 for its nuclear import (and likely for its proper functioning), we inferred that block of MoCks1 nuclear import in the *mokap119*Δ mutant may also lead to disruption of transcriptional regulation by MoSom1, although MoSom1 did not depend on MoKap119 for its nuclear transport.

To identify the potential target genes subject to transcriptional regulation by MoCks1 -MoSom1, depending on MoKap119 for its nuclear transport, we performed the transcriptome analysis between WT and the *mokap119*Δ mycelia. In the two biological

repeats we totally identified 1462 differentially expressed genes (DEGs, |log2|≥1), with 722 DEGs overlapped (Suppl Dataset 3). The expression level of *MoKAP119* (*MGG_02927*) was significantly reduced (log2=-10.29500358 and -11.44725546 respectively in two sets of samples) in the *mokap119*Δ mutant (Suppl Dataset 3), indicating that the transcriptome result was reliable. The expression level of *MoCKS1*, *MoCDC28*, *MoSOM1*, and three cyclin B encoding genes were not among the DEGs in either set of the samples, indicating that the *mokap119*Δ phenotype was not caused by altered transcription of these genes. The 722 overlapped DEGs were highly enriched in amino acid metabolism, carbon metabolism and lipid metabolism pathways (Suppl Dataset 4 and Fig. S4). We compared the overlapped DEGs from two WT vs *mokap119*Δ sets, with the reported DEGs (|log2|≥1.5) between WT and the *mosom1*Δ [33], and found 44 DEGs in common (Suppl Dataset 5), likely as the target genes of MoCks1-MoSom1 pathway in *M. oryzae*, and responsible for fungal pathogenicity. In summary, our transcriptome analysis revealed a possible mechanism of transcriptional regulation of *M. oryzae* pathogenicity genes, which may be at least partially dependent on MoKap119 importin for nuclear transport of MoCks1 and formation of MoCks1-MoSom1 transcriptional complex.

Discussion

Nucleocytoplasmic transport of shuttling proteins serves crucial cellular and biological functions in eukaryotic cells, as transport carriers and signal transduction regulators act under various physiological conditions [34]. Functions of nuclear importins/karyopherins (Kaps)

were reported in yeasts, plants and animal cells, likely involved in regulation of basic cellular activities including transcription [22], translation [35], spindole pole body duplication [36], miRNA biogenesis [37,38], as well as plant immunity [39,40] and human disease including cancer [41-43] and neurodegenerative diseases [44-46]. In *M. oryzae*, so far only an ortholog of exportin-5/Msn5 (EXP5) was reported as critical for full virulent on rice roots [13]. However, the exact mechanism remains unknown.

Cyclin-dependent kinases (CDKs) are a family of kinases playing a role in cell cycle regulation, when forming an active kinase complex with a regulatory protein called a cyclin [47]. CDKs ubiquitously present in enkaryotic cells and evolutionarily conserved in cell cycle regulation [48]. Besides cyclins, the CDKs also directly associate with Cks, a family of small proteins (9-18 kDa) conserved in yeasts, human cells and *Xenopus* oocytes [47,49]. Cks proteins are required for CDKs function, for example, the *Schizosaccharomyces pombe* Cks gene *SUC1* [50] and its homolog in *S. cerevisiae*, *CKS1* [51], both are required for Cdc2/Cdc28 function in yeast cell cycle regulation; their homologs in human cells, *CKShsl* and *CKShs2*, serve evolutionally conserved function in Cdc28/Cdc2 kinase activity and mitosis regulation [52]. In *M. oryzae*, *CKS1* homologous gene was identified by Yue et. al. and was shown to be essential for hyphal growth, colony pigmentation, conidiation, sexual mating and pathogenicity, likely via interaction and regulation of Cdc28 and/or transcriptional factor Som1 [31]. *M. oryzae* Som1 is a functional homolog of *S. cerevisiae* Flo8, a transcritional factor at downstream of cAMP/PKA signaling pathway and responsible

for pseudohyphal growth [53]. MoSom1 was reported to responsible for transcriptional regulation of genes critical for infection-related development in *M. oryzae* [33].

In this study, we identified an ortholog of β-imporin Kap119 in *M. oryzae* and named it as MoKap119. The *mokap119*Δ mutant displayed defects in mycelial growth, pigmentation, conidiation and pathogenicity. We noticed that a small ORF (annotated as *MGG_17923*) is near the 3' terminus of the *MoKAP119* gene, and was constructed as one of the homologous fragments for generation of the *mokap119*Δ mutant (Fig. S1). However, we reason that the observed phenotype of the *mokap119*Δ mutant was unlikely due to potential disruption of *MGG_17923* gene. Firstly, the homologous fragment (1.2 kb) contained the intact *MGG_17923* gene and the homologous recombination (to replace *MoKAP119* with *HPT*) did not seem to disrupt promoter or coding region of *MGG_17923*. On the other hand, our transcriptome analysis did not find significant changes in transcription of *MGG_17923*, or other neighbouring genes, *MGG_02928* or *MGG_02926*, in the *mokap119*Δ mutant compared to WT (Suppl Dataset 3). Also, genetic complementation of the *mokap119*Δ mutant with the ectopic *MoKAP119-GFP* fully restored all the observed defects, confirming that *MoKAP119* is responsible for *M. oryzae* mycelial growth and pigmentation, conidiation and pathogenicity.

Yeast importins have been reported to mediate nucleocytoplasmic shuttling of proteins by binding with cargo's nuclear localization signals (NLS) [14, 15]. Nuclear translocation of

Hog1 MAPK was reported to be mediated by the β-importin Nmd5/Kap119 upon osmotic stress, in *S. cerevisiae* [17]. Deletion of the *HOG1* homologous gene in *M. oryzae* resulted in around 10-fold reduction in conidiation, while no obvious defect in mycelia growth in standard growth medium, neither was it defective in appressorium function or host infection [28]. Therefore we infer that the defects in mycelia growth, conidiation and pathogenicity of the *mokap119*Δ mutant was not due to disrupted nuclear import (if any) of Hog1; although we did not examined sub-cellular localization of Hog1 and its dependency on MoKap119 in this study. Another reported cargo of yeast Nmd5/Kap119, the transcription factor TFIIS [18], was not in our MoKap119-IP protein list. Its interaction with MoKap119, and its biological function, awaits future investigation.

In this study, we identified the cyclin dependent kinase regulator MoCks1 [26] as a cargo protein of MoKap119 importin. By cNLS Mapper (http://nls-mapper.iab.keio.ac.jp/cgi-bin/NLS_Mapper_form.cgi), we predicted two potential, overlapped classical NLS (cNLS) sequences,
"KAIPKEYHDSSKGTLKLLWEEEWRGMGITQ" (residue 60-89) and
"KGTLKLLWEEEWRGMGITQSLGWEHYEVHEPE" in the middle region (71-102) of MoCks1. Also, one cNLS was predicted in MoSom1 as "PSPSKRVRLDGGPGF" (236-250), and multiple cNLS in MoCdc28 as follows,
"RIVAMKKIRLEAEDEGVPSTAIREISLLKEMRD" (29-61),
"DGGRGKALPEGTGPQLSRLGLGDTMIKKFM" (100-129),

"DTMIKKFMSQLCDGVRYCHSHRILHRDLKP" (122-151),
"GRQYSTGVDMWSVGCIFAEMCTRKPLFP" (198-225),
"EMCTRKPLFPGDSEIDEIFKIFRL" (216-239), and
"FPKWQRDPNMKLCPGLNDAGLDLLEMMLVY" (264-293). cNLSs are ubiquitously present in nuclear proteins and have been extensively investigated. Recognition and binding with cNLS is usually executed by α-importin, which also interacts with β-importin through its importin-β binding domain (IBB) to form a complex [14, 15]. More recent study revealed that quite a lot of nuclear proteins could also bypass the requirement of α-importin for their nuclear import, but directly interact with β-importins [54, 55]. Such β-importin binding NLS sequence have not been fully elucidated but a consensus motif of "R/K/H-X(2-5)-P-Y" has been proposed based on study with hnRNPA1 family protein M9 [56]. Interestingly, we found one such PY-NLS motif only in MoCdc 28 ("KQACNHPY" residue 302- 309) but not in the other two proteins. We hypothesize that MoCks1, MoCdc28 and MoSom1 may depend on different importin-α/β complexes for their nuclear import, especially when multiple NLS motifs are present in one single protein, and there may be a functional redundancy between different importin complexes. This may explain why MoCks1 lost its nuclear localization in *mokap119*Δ mutant while the other two proteins did not. For MoCdc28, we propose that beside classical nuclear import pathway, it may also be transported solelyby a β-importin, given that a PY-NLS was predicted at its C-terminus. It would be worth pursuing the detailed molecular and cellular mechanisms underlying nucleocytoplasmic shuttling of proteins mediated via importin family in filamentous/pathogenic fungi, and deciphering the corresponding importin (complex) for specific cargo protein.

Among the differentially expressed genes (DEGs) between WT vs *mokap119*Δ mutant (Suppl Dataset 3) overlapped with the reported [33] SAGE analysis between WT and the *mosom1*Δ, we found 44 common DEGs (Suppl Dataset 5), potentially as the target genes regulated by the MoCks1-MoSom1 transcriptional complex. Among them we noticed the presence of a reported *CDA4* gene (*MGG_08774*) encoding a chitin deacetylase responsible for deacetylating chitin in the hyphae at colony margins in *M. oryzae*, but vegetative growth or pathogenic development was largely unaffected in this *cda4*Δ mutant [57]. Another chitin deacetylase, Cbp1 (MGG_12939), is necessary for *M. oryzae* appressorium formation [58] but not among the DEGs of WT vs *mokap119*Δ mutant. We are also interested in the gene encoding a LysM domain-containing protein (*MGG_07571*). As LysM effectors contribute to fungal virulence [59-61], or it could act in cell wall turnover or plant defense [62], this LysM domain-containing protein would be of interest to further investigation on its function in *M. oryzae* pathogenicity, and the possible regulation by MoCks1-MoSom1.

Whether the observed defects of the *mokap119*Δ mutant is (at least partially) due to failure of activation of MoSom1 transcriptional factor, by MoCks1 which depends on MoKap119 for its nuclear transport, awaits to be unambiguously answered by characterization of the *mokap119*Δ or *mocks1*Δ mutant with a constitutively activated MoSom1. Unfortunately it has not been reported which residue (and modification) of yeast Som1 homolog (named Flo8) makes a dominant-positive mutation of this protein.

Overall, we found physical interaction between MoKap119 and MoCks1. We demonstrated that MoCks1 depends on MoKap119 for its nuclear import, suggesting that the phenotypes observed in the *mokap119*Δ mutant may due to disrupted nuclear translocation of MoCks1. We proposed that failure in nuclear import of MoCks1 may lead to inactivation of Cdc28 kinase activity essential for mitosis, and/or disruption in MoSom1 regulation of gene transcription critical for infection-related development. Our study provides a novel insight into the regulatory mechanism of nucleocytoplasmic shuttling of protein(s) mediated by the β-importin MoKap119, which is essential for fungal development and pathogenicity.

Materials and Methods

Sequence alignment and phylogenetic analysis

The MoKap119 protein sequence was downloaded from the *M.oryzae* online database (https://www.broadinstitute.org/annotation/genome/magnaporthe_grisea). Nmd5/Kap119 orthologous sequences from several organisms were obtained from NCBI database (https://www.ncbi.nlm.nih.gov/). Amino acid sequence alignment was made using the CLUSTAL_W programs and the calculated phylogenetic tree was constructed by MEGA 7.0 program.

Fungal strains and culture conditions

The *M. oryzae* wild type strain B157 (*MAT1-2*) and all transformants generated in this study were cultured on Prune-agar (PA) medium or complete medium (CM) at 28 °C and stored on Whatman filter paper at -20 °C as described [63]. Protoplasts preparation and transformation were conducted as reported previously [64]. For extracting the DNA, RNA and protein, fungal mycelia were harvested after inoculation in liquid CM for 2 days.

Plasmid constructs and fungal transformants

To generate *mokap119*Δ deletion mutants, a 1.2 kb upstream fragment and 1.2 kb downstream fragment of the targeted ORF were respectively amplified from the *M. oryzae* genome using the primer sets listed in Table S1, and ligated sequentially into the *Agrobacterium* Transfer-DNA vector pFGL821 to flank the hygromycin B phsphotransferase cassette (*HPT*). The resulting plasmid was then transferred into the *M. oryzae* wild type strain B157 through *Agrobacterium tumefaciens*-mediated transformation as described previously [10]. To identify the targeted gene deletion mutants, all hygromycin-resistant transformants were first screened by PCR using primers listed in Table S1. The positive transformants were then confirmed by southern blot analysis.

For complementation of *mokap119*Δ mutant and MoKap119 protein localization, we generated the *MoKAP119-GFP* fusion construct. The fragment containing the full-length

coding region of *MoKAP119* (except stop codon) and its 1.5 kb native promoter region was amplified using primers *MoKAP119*-comF/ *MoKAP119*-comR (Table S1) and cloned into *Xho*I-digested pYF11 by the yeast gap repair approach [65]. The *MoKAP119-GFP* fusion construct recovered from yeast Trp+ transformants was confirmed by sequencing analysis, and transformed into the *mokap119*Δ deletion mutant D9 through PEG-mediated transformation. The bleomycin-resistant transformants were evaluated by RT-PCR (primers as listed in Table S1) and examined for GFP signals, to verify the complemented strain D9-C1 and D9-C2.

For construction of the *MoCDC28-GFP*, *MoCKS1-GFP*, *Cyclin B* (*MGG_07065*)-*GFP*, *Cyclin B* (*MGG_05646*)-*GFP*, *Cyclin B1* (*MGG_03595*)-*GFP* and *MoSOM1-GFP* expression plasmids, the fragment containing the full-length coding region of respective gene (except stop codon) with its native promoter region (about 1.5 kb) was amplified using primers listed in Table S1, and then ligated into *Xho*I-digested pCB1532 by ClonExpress II one Step Cloning Kit (Vazyme, C112-01), respectively. The resultant expression constructs were transformed into the wild type B157 and *mokap119*Δ mutant D9, respectively, through PEG-mediated transformation. The sulfonyl urea-resistant transformants were examined by epiflurescence microscopy (Zeiss Observer Z1, Germany).

Assessment of fungal growth, sporulation, appressorium-like structure formation

For vegetative growth assay, equal-sized plugs of each strain were cultivated on CM agar or PA medium at 28 °C for 1 week, and the radial of colonies was measured to calculate radial growth of vegetative mycelia as previously described [66].

Conidia were harvested from 7-d-old cultures, and quantified as previously reported [10]. Appressorium-like structure formation assay was performed following an established protocol [67]. All treatments were performed in three independent biological experiments with three replicates. The significance analysis was performed using *t*-test formula in Excel software.

Pathogenicity assays

Plant infection assays were performed on 7-day-old barley leaves cv *Golden Promise* or 14-day-old rice cv CO-39 seedlings, both highly susceptible toward *M. oryzae*. Mycelial plugs of indicated strains were placed onto intact or wounded barley leaves or rice leaves. Inoculated leaves were kept in a high humidity at 28 °C in darkness for the first 24 h, followed by a 12 h: 12 h, light: dark cycle. Root infection assay of rice was performed on 2% water agar plate as previously described [33]. Each assay was repeated three times. The disease severity was assessed at 5 d after inoculation.

Nucleic acid manipulation and Southern blot analysis

Genomic DNA of each isolates was extracted from mycelia using a fungal DNA Midi Kit (Omega, D3590-01). The resulting genomic DNA was used for PCR screening or Southern blot hybridization. 10 μg genomic DNA of indicated strains were digested with restriction enzyme(s). Digested products were eletrophoresed in a 1% agarose gel and then transferred onto Hybond-N^+ membrane (Amersham). 5' flank sequence of *MoKAP119* was used as the specific probe, which was labeled with digoxigenin-11-dUTP using DIG-High prime according to the manufacture's instructions (Roche, 11745832910). Hybridization and detection were performed according to the instruction manual (Roche Applied Science). Total RNA isolation from the mycelia was performed using RNeasy Mini Kit (Qiagen, 74104). Total RNA was treated with DNase (Invitrogen, 18047019) and verified as DNA free by using them as template in a PCR assay. First-strand cDNA was synthesized according to the instruction manual (ThermoFisher Scientific, K1622).

RT-PCR and Real Time qRT-PCR analysis

RT-PCR or qRT-PCR was performed using cDNA as a template. RT-PCR was carried out to confirm the deletion or reintroduction of *MoKAP119* gene with the prime pairs *MoKAP119*-F/*MoKAP119*-R. qRT-PCR was performed with a Power SYBR Green PCR Master Mix Kit (Applied biosystems, 4367659) using an ABI QuantStudio ^{TM} 7 Flex system according to the manufacturer's instructions. Both RT-PCR and qRT-PCR were conducted in triplicates for each sample and the experiment was repeated three times. The gene

MGG_00604, encoding *M. oryzae* beta-tubulin, was used as an endogenous reference. All primers used in this study are listed in Table S1.

Epifluorescence microscopy and staining

M. oryzae cells expressing fluorescent protein-fused chimera were grown under requisite conditions. Epifluorescence microscopy was performed using Observer Z1 equipped with sCMOS camera (PCO Edge, Germany). To visualize the nucleus, mycelia or conidia were stained with 2 μg/ml Hoechst 3342 (Thermo Scientific, 62249) at room temperature for 10 min, followed by three washes with PBS, then viewed under the epifluorescence microscope.

Affinity purification and MS analysis

The MoKap119-GFP fusion construct was transformed into the wild-type B157 and *mokap119*Δ deletion mutant D9. The expression of MoKap119-GFP protein was confirmed by western blot analysis with an anti-GFP antibody (Abmart). Methods of affinity purification was performed as previously described [66]. LC-MS/MS analysis was carried out by Shanghai Applied Protein Technology Co. Ltd (Shanghai, China), following the established protocol [66].

Transcriptome analysis

Total RNA from WT or D9 strain was extracted using Qiagen RNAeasy Mini kit (Qiagen, 74104) according to the manufacture's protocol, and was then enriched by Oligo(dT) beads. The enriched mRNA was fragmented as 200 nt -700 nt and reverse transcripted into cDNA with random primers. Second-strand cDNA was synthesized by DNA polymerase I, RNase H, dNTP and buffer, and then purified with QiaQuick PCR extraction kit, end repaired, poly (A) added, and ligated to Illumina sequencing adapters. The ligation products were size selected by agarose gel electrophoresis, PCR amplified, and sequenced using Illumina HiSeq TM 2500 by Gene Denovo Biotechnology Co. (Guangzhou, China).

The edgeR package (http://www.r-project.org/) was used for differential expression analysis. Genes with a fold change≥2 and a false discovery rate (FDR) <0.05 in a comparison as significant DEGs were subjected to enrichment analysis of GO functions using the Gene Ontology database (http://www.geneontology.org/), and KEGG pathways using the major public pathway-related database KEGG [68]. The calculating formula of p-value is:

$$P = 1 - \sum_{i=0}^{n-1} \frac{\binom{M}{i}\binom{N-M}{n-i}}{\binom{N}{n}}$$

Where N is the number of all genes that with annotation in database, n is the number of DEGs in N, M is the number of all genes annotated to specific pathways, and m is the number of DEGs in M. The calculated p-value were gone through FDR Correcttion, taking FDR≤

0.05 as a threshold. Q-Value is the P-value after the multiple hypothesis test correction, in the range of 0 to 1, the closer to zero, the more significant the enrichment [69].

Yeast two-hybrid assays

The bait constructs were generated by cloning *MoKAP119* full-length cDNA into pGADT7 (Clontech). The *MoCDC28*, *MoCKS1* or *MoSOM1* cDNA was respectively cloned into pGBKT7 (Clontech) as the prey construct. All primers were listed in Table S1. The resulting bait and prey constructs were confirmed by sequencing analysis, then transformed into yeast Y2H Gold following the manufacturer's instructions (MATCHMAKER Gold Yeast Two-Hybrid System).

Co-immunoprecipitation

Gonomic locus of *MoCDC28*, including 1.5 kb native promoter and ORF region without stop codon, was cloned into pHZ126-3xFlag vector. The resulting vector MoCdc28-3xFlag was alone or co-transformed with MoKap119-GFP (constructed as described above) into the wild-type protoplasts. The total proteins were isolated from correct transformants and incubated with GFP_Trap A (Chromotek, gta-20). Proteins bound to GFP-trap beads were eluted after a series of washing steps following manufacture's instruction. Western blot analysis of total proteins and Co-IP proteins was performed using anti-FLAG (Sigma Aldrich) or anti-GFP (Abmart) antibody, and detected using the ECL supersignal system (Pierce,

Rockford, IL).

.

Acknowledgements

This work was supported by the National Basic Research Program of China (973 Program, grant number 2015CB150600), and Guangdong Province Science and Technology Innovation Strategy Special Fund (2018B020206001). We are grateful to Prof. Zhengguang Zhang of Nanjing Agricultural University and Prof. Zhengyi Wang of Zhejiang Univesity for providing pYF11, pHZ126 and pCB1532 vectors. We also thank Prof. Jianping Lu of Zhejiang University, Prof. Min Guo of Anhui Agricultural University and Dr. Muxing Liu of Nanjing Agricultural University for technical assistance. We thank the Shanghai Applied Protein Technology Co. Ltd for technology support in Mass Spectrometry identification of immunoprecipitated proteins. We thank the GENE DENOVO company for transcriptome analysis.

Author Contributions

YZ. Deng, and LH. Zhang conceived and designed the experiments; S. Zhang, C. Lin and T. Zhou performed the experiments; YZ. Deng, and S. Zhang analyzed the data and wrote the manuscript.

Conflict of Interest

The authors have no competing financial interests and are solely responsible for the experimental designs and data analysis.

Reference

1. Horbach R, Navarro-Quesada AR, Knogge W, Deising HB (2011) When and how to kill a plant cell: infection strategies of plant pathogenic fungi. J Plant Physiol 168: 51-62.

2. Yan X, Talbot NJ (2016) Investigating the cell biology of plant infection by the rice blast fungus Magnaporthe oryzae. Curr Opin Microbiol 34: 147-153.

3. Kamoun S, Furzer O, Jones JD, Judelson HS, Ali GS, et al. (2015) The Top 10 oomycete pathogens in molecular plant pathology. Mol Plant Pathol 16: 413-434.

4. Lee K, Singh P, Chung WC, Ash J, Kim TS, et al. (2006) Light regulation of asexual development in the rice blast fungus, Magnaporthe oryzae. Fungal Genet Biol 43: 694-706.

5. Wilson RA, Talbot NJ (2009) Under pressure: investigating the biology of plant infection by Magnaporthe oryzae. Nat Rev Microbiol 7: 185-195.

6. Kumar A, Ghosh S, Nath Bhatt D, Narula A, Datta A (2016) Magnaporthe oryzae aminosugar metabolism is essential for successful host colonization. Environ Microbiol 18: 2768.

7. Goh J, Kim KS, Park J, Jeon J, Park SY, et al. (2011) The cell cycle gene MoCDC15 regulates hyphal growth, asexual development and plant infection in the rice blast pathogen Magnaporthe oryzae. Fungal Genet Biol 48: 784-792.

8. Yang J, Zhao X, Sun J, Kang Z, Ding S, et al. (2010) A novel protein Com1 is required for normal conidium morphology and full virulence in Magnaporthe oryzae. Mol Plant Microbe Interact 23: 112-123.

9. Kong LA, Yang J, Li GT, Qi LL, Zhang YJ, et al. (2012) Different chitin synthase genes are required for various developmental and plant infection processes in the rice blast fungus Magnaporthe oryzae. PLoS Pathog 8: e1002526.

10. Deng YZ, Qu Z, He Y, Naqvi NI (2012) Sorting nexin Snx41 is essential for conidiation and mediates glutathione-based antioxidant defense during invasive growth in Magnaporthe oryzae. Autophagy 8: 1058-1070.

11. Li G, Zhou X, Xu JR (2012) Genetic control of infection-related development in

Magnaporthe oryzae. Curr Opin Microbiol 15: 678-684.

12. DeZwaan TM, Carroll AM, Valent B, Sweigard JA (1999) Magnaporthe grisea pth11p is a novel plasma membrane protein that mediates appressorium differentiation in response to inductive substrate cues. Plant Cell 11: 2013-2030.

13. Tucker SL, Besi MI, Galhano R, Franceschetti M, Goetz S, et al. (2010) Common genetic pathways regulate organ-specific infection-related development in the rice blast fungus. Plant Cell 22: 953-972.

14. Caesar S, Greiner M, Schlenstedt G (2006) Kap120 functions as a nuclear import receptor for ribosome assembly factor Rpf1 in yeast. Mol Cell Biol 26: 3170-3180.

15. Kimura M, Imamoto N (2014) Biological significance of the importin-beta family-dependent nucleocytoplasmic transport pathways. Traffic 15: 727-748.

16. Ohno M, Fornerod M, Mattaj IW (1998) Nucleocytoplasmic transport: the last 200 nanometers. Cell 92: 327-336.

17. Ferrigno P, Posas F, Koepp D, Saito H, Silver PA (1998) Regulated nucleo/cytoplasmic exchange of HOG1 MAPK requires the importin beta homologs NMD5 and XPO1. EMBO J 17: 5606-5614.

18. Albertini M, Pemberton LF, Rosenblum JS, Blobel G (1998) A novel nuclear import pathway for the transcription factor TFIIS. J Cell Biol. 143(6):1447-55.

19. Fernandez-Cid A, Vega, M., Herrero, P., Moreno, F. (2012) Yeast importin-β is required for nuclear import of the Mig2 repressor. BMC Cell Biology 13.

20. Martinez-Bono B, Quilis I, Zalve E, Igual JC (2010) Yeast karyopherins Kap123 and Kap95 are related to the function of the cell integrity pathway. FEMS Yeast Res 10: 28-37.

21. Taberner FJ, Igual JC (2010) Yeast karyopherin Kap95 is required for cell cycle progression at Start. BMC Cell Biol 11: 47.

22. Taberner FJ, Quilis I, Sendra J, Bano MC, Igual JC (2012) Regulation of cell cycle transcription factor Swi5 by karyopherin Msn5. Biochim Biophys Acta 1823: 959-970.

23. Markina-Iñarrairaegui A, Etxebeste O, Herrero-García E, Araújo-Bazán L, Fernández-Martínez J, Flores JA, Osmani SA, Espeso EA (2011) Nuclear transporters in a multinucleated organism: functional and localization analyses in Aspergillus nidulans. Mol Biol Cell. 22(20):3874-86.

24. Etxebeste O, Markina-Iñarrairaegui A, Garzia A, Herrero-García E, Ugalde U, Espeso EA (2009) KapI, a non-essential member of the Pse1p/Imp5 karyopherin family, controls colonial and asexual development in Aspergillus nidulans. Microbiology. 155(Pt 12):3934-45.

25. Araújo-Bazán L1, Dhingra S, Chu J, Fernández-Martínez J, Calvo AM, Espeso EA (2009) Importin alpha is an essential nuclear import carrier adaptor required for proper sexual

and asexual development and secondary metabolism in Aspergillus nidulans. Fungal Genet Biol. 46(6-7):506-15.

26. Bernardes NE, Takeda AAS, Dreyer TR, Cupertino FB, Virgilio S, et al. (2017) Nuclear transport of the Neurospora crassa NIT-2 transcription factor is mediated by importin-alpha. Biochem J 474: 4091-4104.

27. Ghassemi S, Lichius A, Bidard F, Lemoine S, Rossignol MN, et al. (2015) The β-importin KAP8 (Pse1/Kap121) is required for nuclear import of the cellulase transcriptional regulator XYR1, asexual sporulation and stress resistance in Trichoderma reesei. Mol Microbiol 96: 405-418.

28. Dixon KP, Xu JR, Smirnoff N, Talbot NJ. Independent signaling pathways regulate cellular turgor during hyperosmotic stress and appressorium-mediated plant infection by Magnaporthe grisea. Plant Cell 11(10):2045-58.

29. Howard R, Valent, B. (1996) BREAKING AND ENTERING: Host Penetration by the Fungal Rice Blast Pathogen Magnaporthe grisea. Annu Rev Microbiol 50: 491 – 512.

30. Talbot NJ (2003) On the trail of a cereal killer: Exploring the biology of Magnaporthe grisea. Annu Rev Microbiol 57: 177-202.

31. Yue X, Que Y, Deng S, Xu L, Oses-Ruiz M, et al. (2017) The cyclin dependent kinase subunit Cks1 is required for infection-associated development of the rice blast fungus Magnaporthe oryzae. Environ Microbiol 19: 3959-3981.

32. Martinsson-Ahlzen HS, Liberal V, Grunenfelder B, Chaves SR, Spruck CH, et al. (2008) Cyclin-dependent kinase-associated proteins Cks1 and Cks2 are essential during early embryogenesis and for cell cycle progression in somatic cells. Mol Cell Biol 28: 5698-5709.

33. Yan X, Li Y, Yue X, Wang C, Que Y, et al. (2011) Two novel transcriptional regulators are essential for infection-related morphogenesis and pathogenicity of the rice blast fungus Magnaporthe oryzae. PLoS Pathog 7: e1002385.

34. Fu X, Liang C, Li F, Wang L, Wu X, et al. (2018) The Rules and Functions of Nucleocytoplasmic Shuttling Proteins. Int J Mol Sci 19.

35. Veenhoff LM, Meinema AC, Poolman B (2010) A karyopherin acts in localized protein synthesis. Cell Cycle 9: 1281-1285.

36. Kupke T, Di Cecco L, Muller HM, Neuner A, Adolf F, et al. (2011) Targeting of Nbp1 to the inner nuclear membrane is essential for spindle pole body duplication. EMBO J 30: 3337-3352.

37. Cui Y, Fang X, Qi Y (2016) TRANSPORTIN1 Promotes the Association of MicroRNA with ARGONAUTE1 in Arabidopsis. Plant Cell 28: 2576-2585.

38. Zhang Z, Guo X, Ge C, Ma Z, Jiang M, et al. (2017) KETCH1 imports HYL1 to nucleus for miRNA biogenesis in Arabidopsis. Proc Natl Acad Sci U S A 114: 4011-4016.

39. Roth C, Ludke D, Klenke M, Quathamer A, Valerius O, et al. (2017) The truncated NLR protein TIR-NBS13 is a MOS6/IMPORTIN-alpha3 interaction partner required for plant immunity. Plant J 92: 808-821.

40. Ludke D, Roth C, Hartken D, Wiermer M (2018) MOS6 and TN13 in plant immunity. Plant Signal Behav 13: e1454816.

41. Mandic R, Schamberger CJ, Muller JF, Geyer M, Zhu L, et al. (2005) Reduced cisplatin sensitivity of head and neck squamous cell carcinoma cell lines correlates with mutations affecting the COOH-terminal nuclear localization signal of p53. Clin Cancer Res 11: 6845-6852.

42. Cagatay T, Chook YM (2018) Karyopherins in cancer. Curr Opin Cell Biol 52: 30-42.

43. Zhao J, Shi L, Zeng S, Ma C, Xu W, et al. (2018) Importin-11 overexpression promotes the migration, invasion, and progression of bladder cancer associated with the deregulation of CDKN1A and THBS1. Urol Oncol 36: 311 e311-311 e313.

44. Kim HJ, Taylor JP (2017) Lost in Transportation: Nucleocytoplasmic Transport Defects in ALS and Other Neurodegenerative Diseases. Neuron 96: 285-297.

45. Da Cruz S, Cleveland DW (2016) CELL BIOLOGY. Disrupted nuclear import-export in neurodegeneration. Science 351: 125-126.

46. Lee HG, Ueda M, Miyamoto Y, Yoneda Y, Perry G, et al. (2006) Aberrant localization of importin alpha1 in hippocampal neurons in Alzheimer disease. Brain Res 1124: 1-4.

47. Morgan DO (1997) CYCLIN-DEPENDENT KINASES: Engines, Clocks, and Microprocessors. Annu Rev Cell Dev Biol 13: 261-291.

48. Morgan DO (2007) The Cell Cycle: Principles of Control: New Science Press.

49. Pines J (1996) Cell cycle: Reaching for a role for the Cks proteins. Current Biology 6: 1399-1402.

50. Hayles J, Beach D, Durkacz B, Nurse P (1986) The fission yeast cell cycle control gene cdc2: isolation of a sequence sucl that suppresses cdc2 mutant function. Mol Gen Genet 202: 291-293.

51. Hadwiger JA, Wittenberg C, Mendenhall MD, Reed SI (1989) The Saccharomyces cerevisiae CKS1 gene, a homolog of the Schizosaccharomyces pombe suc1+ gene, encodes a subunit of the Cdc28 protein kinase complex. Mol Cell Biol 9: 2034-2041.

52. Richardson HE, Stueland CS, Thomas J, Russell P, Reed SI (1990) Human cDNAs encoding homologs of the small p34Cdc28/Cdc2-associated protein of Saccharomyces cerevisiae and Schizosaccharomyces pombe. Genes Dev 4: 1332-1344.

53. Liu H, Styles CA, Fink GR (1996) Saccharomyces cerevisiae S288C has a mutation in FLO8, a gene required for filamentous growth. Genetics 144: 967-978.

54. Bonifaci N, Moroianu J, Radu A, Blobel G. Karyopherin beta2 mediates nuclear import of a mRNA binding protein. Proc Natl Acad Sci U S A 94(10):5055-60.

55. Moroianu J. Distinct nuclear import and export pathways mediated by members of the karyopherin beta family. J Cell Biochem 70(2):231-9.

56. Bonifaci N, Moroianu J, Radu A, Blobel G. Karyopherin beta2 mediates nuclear import of a mRNA binding protein. Proc Natl Acad Sci U S A. 1997 May 13;94(10):5055-60.

57. Geoghegan IA, Gurr SJ (2017) Investigating chitin deacetylation and chitosan hydrolysis during vegetative growth in Magnaporthe oryzae. Cell Microbiol. 19(9).

58. Kuroki M, Okauchi K, Yoshida S, Ohno Y, Murata S, Nakajima Y, Nozaka A, Tanaka N, Nakajima M, Taguchi H, Saitoh KI, Teraoka T, Narukawa M, Kamakura T. Chitin-deacetylase activity induces appressorium differentiation in the rice blast fungus Magnaporthe oryzae. (2017) Sci Rep. 7(1):9697.

59. Cen K, Li B, Lu Y, Zhang S, Wang C (2017) Divergent LysM effectors contribute to the virulence of Beauveria bassiana by evasion of insect immune defenses. PLoS Pathog. 13(9):e1006604.

60. Koharudin LM, Debiec KT1, Gronenborn AM. (2015) Structural Insight into Fungal Cell Wall Recognition by a CVNH Protein with a Single LysM Domain. Structure. 23(11):2143-54.

61. Mentlak TA, Kombrink A, Shinya T, Ryder LS, Otomo I, Saitoh H, Terauchi R, Nishizawa Y, Shibuya N, Thomma BP, Talbot NJ. (2012) Effector-mediated suppression of chitin-triggered immunity by magnaporthe oryzae is necessary for rice blast disease. Plant Cell. 24(1):322-35.

62. Koharudin LM, Debiec KT, Gronenborn AM. (2015) Structural Insight into Fungal Cell Wall Recognition by a CVNH Protein with a Single LysM Domain. Structure. 2015 Nov 3;23(11):2143-54.

63. Ramos-Pamplona M, Naqvi NI (2006) Host invasion during rice-blast disease requires carnitine-dependent transport of peroxisomal acetyl-CoA. Mol Microbiol 61: 61-75.

64. Park G, Xue C, Zhao X, Kim Y, Orbach M, et al. (2006) Multiple upstream signals converge on the adaptor protein Mst50 in Magnaporthe grisea. Plant Cell 18: 2822-2835.

65. Zhou X, Li G, Xu JR (2011) Efficient approaches for generating GFP fusion and epitope-tagging constructs in filamentous fungi. Methods Mol Biol 722: 199-212.

66. Zhang S, Liang M, Naqvi NI, Lin C, Qian W, et al. (2017) Phototrophy and starvation-based induction of autophagy upon removal of Gcn5-catalyzed acetylation of Atg7 in Magnaporthe oryzae. Autophagy 13: 1318-1330.

67. Guo M, Gao F, Zhu X, Nie X, Pan Y, et al. (2015) MoGrr1, a novel F-box protein, is involved in conidiogenesis and cell wall integrity and is critical for the full virulence of

Magnaporthe oryzae. Appl Microbiol Biotechnol 99: 8075-8088.

68. Kanehisa M, Araki M, Goto S, Hattori M, Hirakawa M, et al. (2008) KEGG for linking genomes to life and the environment. Nucleic Acids Res 36: D480-484.

69. Shen YH, Lu BG, Feng L, Yang FY, Geng JJ, Ming R, Chen XJ. Isolation of ripening-related genes from ethylene/1-MCP treated papaya through RNA-seq. BMC Genomics 18(1):671.

70. Felsenstein J. (1985). Confidence limits on phylogenies: An approach using the bootstrap. Evolution 39:783-791.

71. Jones DT, Taylor WR, and Thornton JM. (1992). The rapid generation of mutation data matrices from protein sequences. Computer Applications in the Biosciences 8: 275-282.

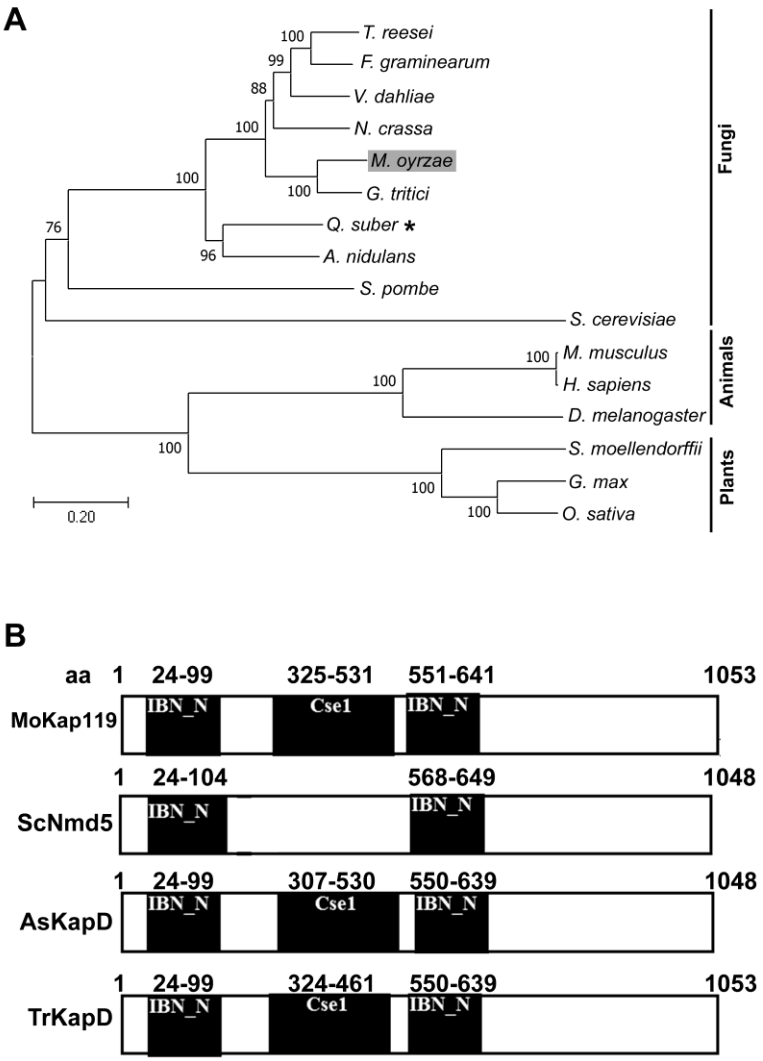

Figure 1 Prediction of domains and phylogenetic analysis of Kap119 homologues in different organisms. (A) Phylogenetic analysis of MoKap119 and its orthologous proteins obtained by BLASTP search from fungal, plant and animal species. The protein sequences used for alignment include: Fungi: XP_003720790.1 (*M. oryzae*, MGG_02927), NP_588103.1 (*S. pombe*), NP_012666.2 (*S. cerevisiae*), XP_009221001.1 (*Gaeumannomyces tritici*), XP_009658102.1 (*Verticillium dahliae*), EYB28655.1 (*Fusarium graminearum*), XP_006964328.1 (*Trichoderma reesei*), XP_964123.1 (*N. crassa*), XP_663610.1 (*A. nidulans*); Animals: NP_006382.1 (*Homo sapiens*), NP_852658.2 (*Mus musculus*), NP_524780.1 (*Drosophila melanogaster*); Plants: XP_023917558.1 (*Quercus suber*), XP_024538469.1 (*Selaginella moellendorffii*), XP_014634734.1 (*Glycine max*), and EEC73155.1 (*Oryza sativa*). Sequence alignment was performed using the CLUSTAL_W and the neighbour-joining tree was constructed by MEGA 7.0 with 1000 bootstrap. The optimal tree with the sum of branch length = 6.14682829 is shown. The percentage of replicate trees in which the associated taxa clustered together in the bootstrap test (1000 replicates) are shown next to the branches [70]. The tree is drawn to scale, with branch lengths in the same units as those of the evolutionary distances used to infer the phylogenetic

tree. The evolutionary distances were computed using the JTT matrix-based method [71] and are in the units of the number of amino acid substitutions per site. All positions with less than 50% site coverage were eliminated. Scale bar represents 20 mutations per 100 residues. The position of MoKap119 in the phylogenetic tree is indicated by the grey highlighting. Askterisk denotes a plant ortholog clustered in fungal clade. (B) Prediction of domains of Kap119/Nmd5/KapD proteins of *M. oryzae*, *S. cerevisiae*, *A. nidulans* and *T. reesei* was performed using the SMART website (http://smart.embl-heidelberg.de/). Amino acid (aa) residue number of the start and end of the protein, as well as the annotated domains, was labeled on the top of the protein. IBN_N: Importin-beta N-terminal domain; Cse1: chromosome segregation 1-like (yeast) domain.

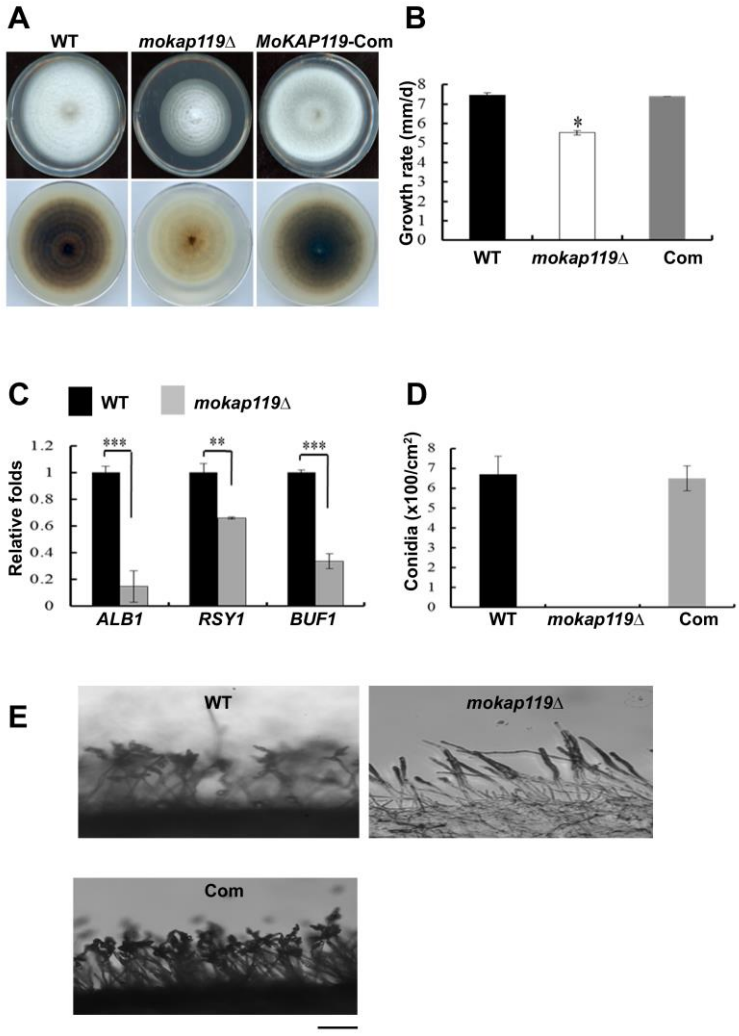

Figure 2 *MoKAP119* is essential for vegetative growth and mycelial pigmentation. (A) Radial growth of wild type (WT), the *mokap119*Δ mutant and complementation strain (*MoKAP119*-Com) grown on complete medium (CM) at 28 °C. Images were taken at 7 day post inoculation, from the top (top panel) and bottom (bottom panel) view of the cultured mycelia respectively. (B) Rate of radial growth was measured and represented as the barchart (Mean ± S.E.; three independent biological replica). Asterisk denotes significant difference (P<0.05). Com, the *MoKAP119* complementation strain. (C) Transcriptional level of three melanin biosynthesis-related gene was analyzed by qRT-PCR. The experiments were performed with three independent biological replicates, each of which contains three replica. Statistical analysis was performed with student's *t*-test. Asterisks represent significant differences from the control (P < 0.01). (D) Bar chart depicting quantitatively assessed conidiation in the *mokap119*Δ mutant and complementation strain (Com) grown on prune-agar (PA) medium. Mean values (±S.E.) were derived from three independent experiments (n = 3 colonies for each sample). Assessments were performed 3 days post induction. (E) Photomicrographs depicting the extent of conidia formation in aforementioned strains. Images were taken 3 days post induction of conidiation. Scale bar = 20 micron.

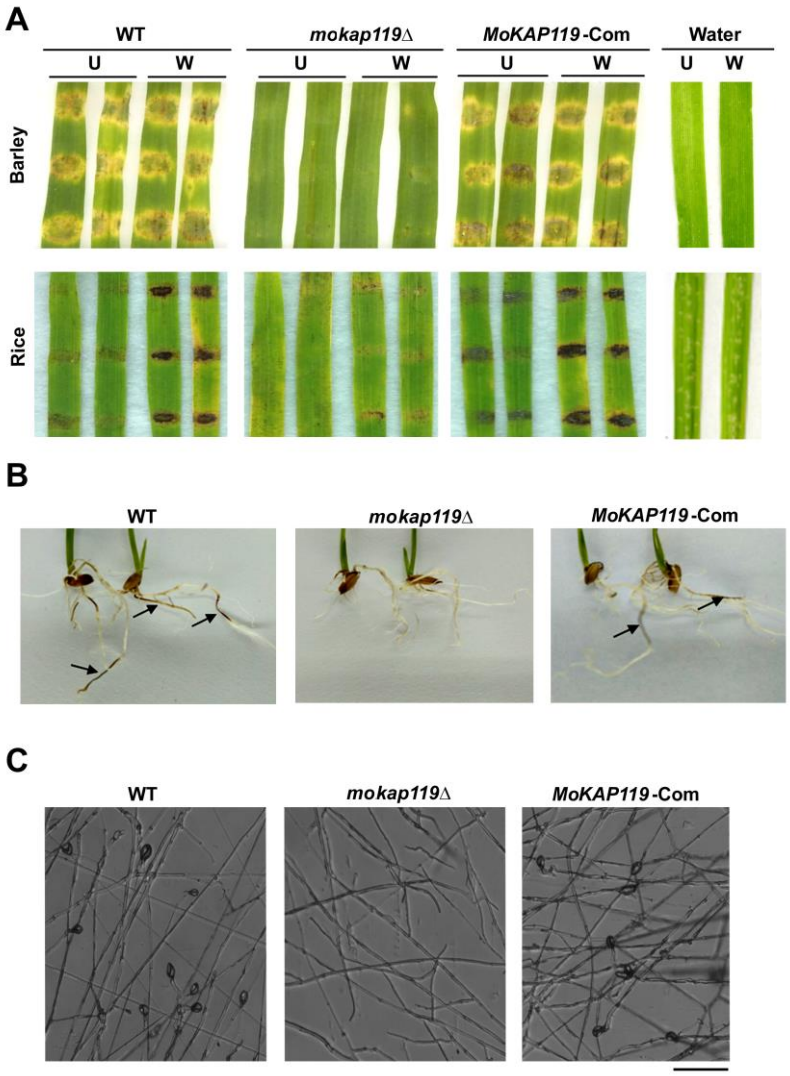

Figure 3 *MoKAP119* is required for *M. oryzae* pathogenicity and appressorium-like structure formation. (A) Pathogenicity was tested on unwounded (U) and wounded (W) barely (upper panel) or rice (lower panel) leaf explants with the mycelial plugs of same size, from WT, the *mokap119*Δ mutant and complementation strain (*MoKAP119*-Com). The inoculated leaves were first kept in dark at 28ºC for 24 h, and then kept in the growth chamber with the setting temperature of 28ºC and dark/light cycle of 12/12 h. Inoculation with water served as blank control. Images were taken at 5 dpi. (B) Root infection assay. The mycelial fragments of indicated strain were placed on rice root. Photographs were taken at 5 days after inoculation. Arrows denote necrotic lesions. (C) Appressorium-like structure formation assay. Mycelial fragments of the tested strain were placed on hydrophobic GelBond film and inoculated in a humid chamber at 28 °C for 24-48 h, before microscopic observation and photographing. Scale bar = 20 micron.

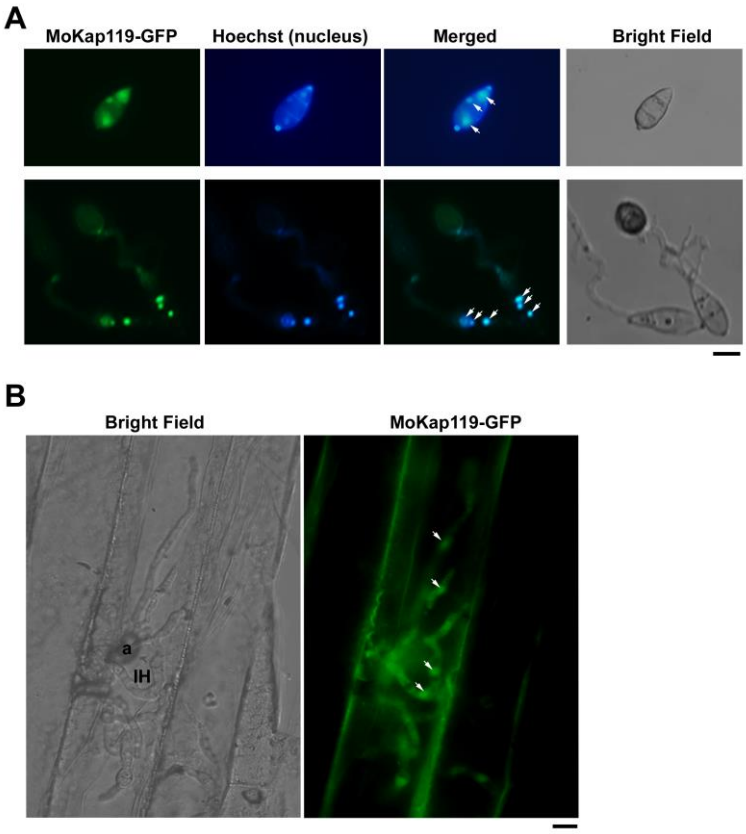

Figure 4 Sub-cellular localization of MoKap119-GFP in *M. oryzae*. (A) The complementation strain carrying MoKap119-GFP was co-stained with the nuclear fluorescent dye Hoechst 33342 (Thermo Scientific, 62249) and imaged with epifluorescence microscopy, for conidia at 0 h (upper panel) or 12 h (lower panel) post inoculation on artificial inductive surface. Scale bar = 5 μm. (B) Sub-cellular localization of MoKap119-GFP during invasive growth in barely explantes. Photographs were taken at 48 h post incubation (hpi). a = appressorium; IH = invasive hypha. Scale bar = 5 μm.

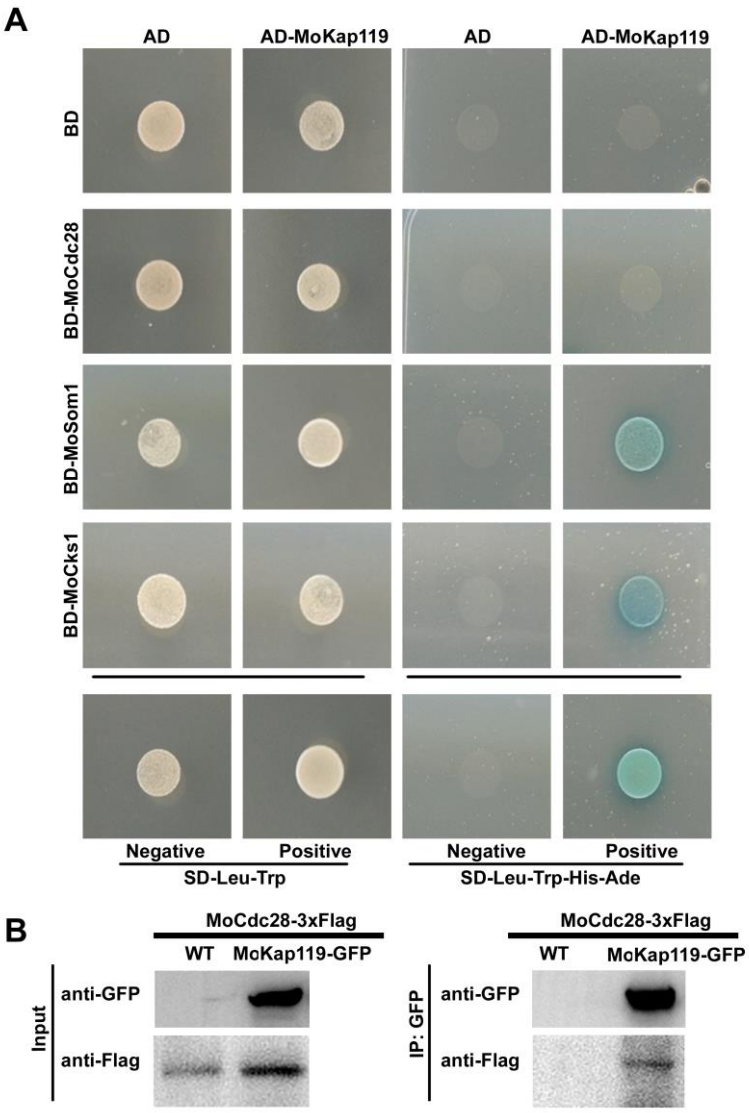

Figure 5 MoKap119 directly interacts with MoCks1, MoSom1 and MoCdc28. (A) Yeast two-hybrid assay for the interaction among MoCks1, MoCdc28, MoSom1 and MoKap119. Yeast transformants co-transformed with pGADT7-T and pGBKT7-53 was used as positive control, and co-transformed with pGADT7-T and pGBKT7-Lam as negative control. (B) Co-immunoprecipitation assays between MoCdc28 and MoKap119. The wild-type strains containing MoKap119-GFP, or MoKap119-GFP and MoCdc28-3 x FLAG, were grown in liquid CM at 28 ºC for 48 h. Total proteins extracted from the strains were subjected to 12% SDS-PAGE and immunoblots were incubated with anti-GFP or anti-FLAG antibody respectively. The total protein samples were pulled down using GFP_Trap A (Chromotek, gta-20) and then detected with anti-GFP or anti-FLAG antibody.

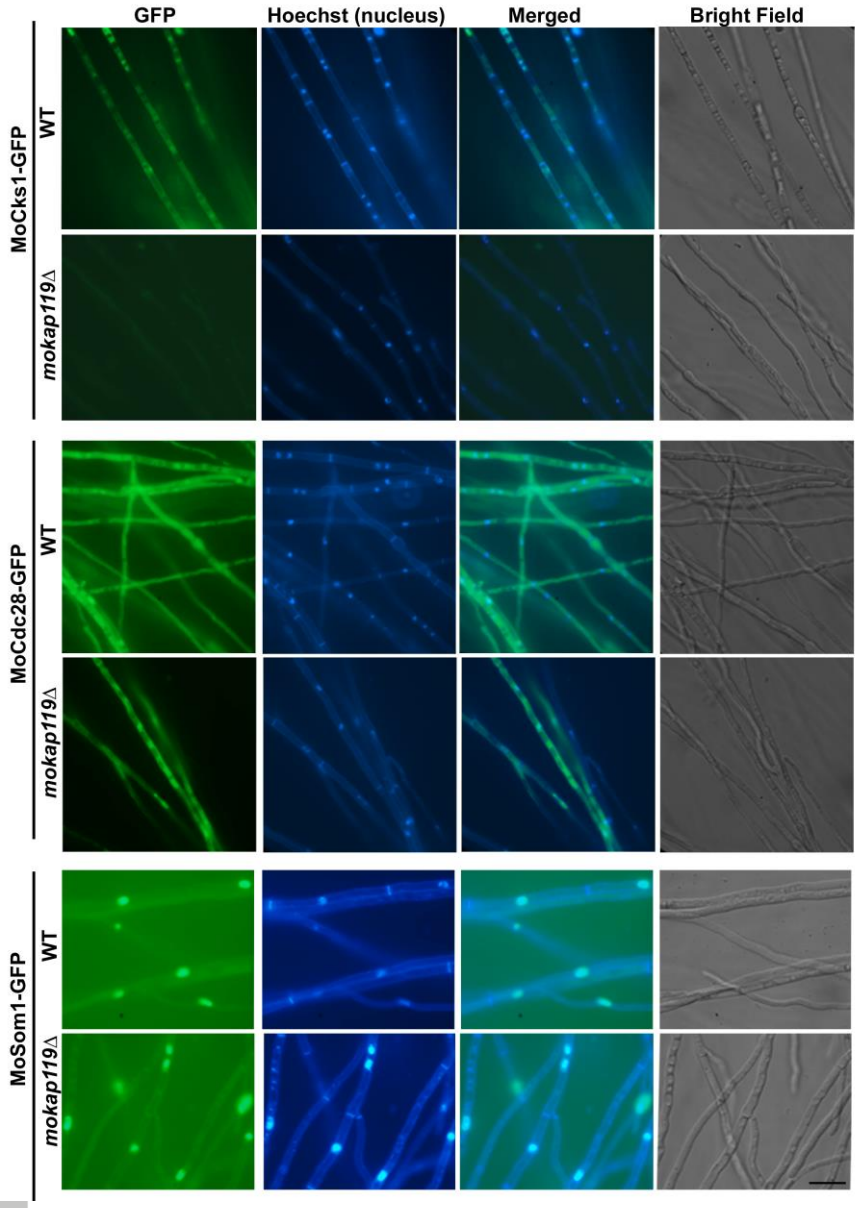

Figure 6 Sub-cellular localization of MoCks1-GFP, MoSom1-GFP and MoCdc28-GFP in wild type (WT) or *mokap119*Δ mycelia. The mycelia of the strains carrying MoCks1-GFP, MoSom1-GFP or MoCdc28-GFP were cultured in CM medium and subject to epifluorescence microscopy and imaging. Scale bar = 5 μm.

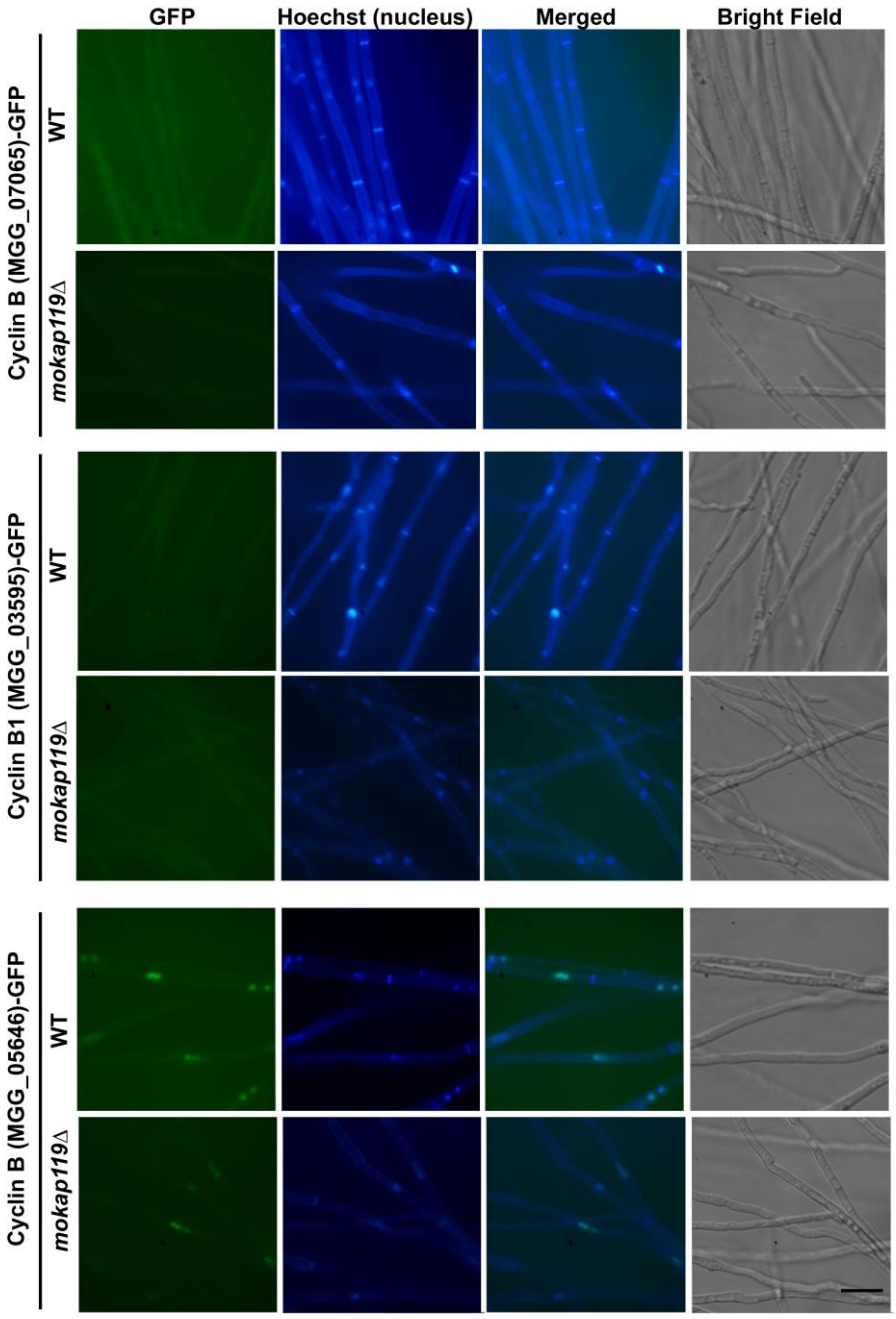

Figure 7 Sub-cellular localization of Cyclin B orthologs in wild type (WT) or *mokap119*Δ mycelia. Three Cyclin B proteins in *M. oryzae* were tagged with GFP at their C-terminus respectively. The mycelia of these strains were cultured in CM medium and subject to epifluorescence microscopy and imaging. Scale bar = 5 μm.